

Statistical Analysis of Impact Points of Rockets

By

Yasunori MATOGAWA, Motoki HINADA and Kohko FUKUDA

Summary: Data of impact points obtained from rocket vehicles launched at KSC (the Kagoshima Space Center, University of Tokyo) are statistically analyzed on the basis of the normal bivariate distribution method. Results obtained by the binormal method are compared with those obtained by the empirical method. Circular distribution method is shown to be valid if the level of significance is appropriately chosen. Some computations related to the determination of impact zones are carried out.

1. INTRODUCTION

On the firing of rockets, it is required to determine launch angles or impact zones based on the information of the probability of falling on an area of aim, or, conversely the chances of falling outside a specified area due to several undefined factors. Those factors, which cause rockets to fall in different area from the aimed one, are vehicle misalignments, error of estimation on time variation of wind components and so on.

From this viewpoint, it is very important to extract certain statistical informa-

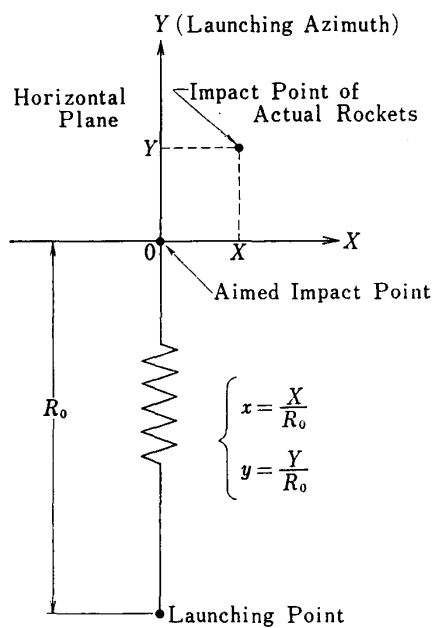


FIG. 1. Coordinate system

tion from available data and also to estimate statistical parameters of the data distribution.

For the statistical treatment of impact point data, the coordinate system O- xy shown in Fig. 1 is used. Then the distribution of impact points may be adequately described by the general bivariate distribution. Continued efforts on the part of many individuals and organizations have resulted in the successful applications of the binormal elliptical distribution to wind distributions [1-3]. The following discussion pertains to those methods and their application to impact point distributions of rockets launched at KSC.

2. COMPUTATION PROCEDURES

2.1 General Two-Dimensional Vector Statistics

A homogeneous two-dimensional vector distribution is said to be normal in the general bivariate sense if the probability density function $f(x, y)$ has the following form:

$$f(x, y) = \frac{1}{2\pi\sigma_x\sigma_y\sqrt{1-\rho^2}} \exp\left(-\frac{C}{2}\right) \quad (1)$$

where

$$C = \frac{1}{1-\rho^2} \left\{ \left(\frac{x-\mu_x}{\sigma_x} \right)^2 - 2\rho \frac{(x-\mu_x)(y-\mu_y)}{\sigma_x\sigma_y} + \left(\frac{y-\mu_y}{\sigma_y} \right)^2 \right\}. \quad (2)$$

In equations (1) and (2), x and y are orthogonal components of statistical vector, μ_x and μ_y are the respective means of the components, σ_x and σ_y are the standard deviations of the respective components and ρ is the correlation coefficient between the components.

In the case where population parameters are not known and also sample size is large enough, μ_x and μ_y are reasonably replaced by their respective estimates \bar{x} and \bar{y} from total collective where the bar indicates an averaging process.

Also, the variances σ_x^2 and σ_y^2 are replaced by their respective estimates s_x^2 and s_y^2 , and for the correlation coefficient ρ , its estimate r is used.

In the case where the component variances, σ_x^2 and σ_y^2 , are equal and the correlation ρ is zero, the distribution is circular and distribution circles may be drawn, centered on the point, (μ_x, μ_y) . Where correlation is present and the component variances, σ_x^2 and σ_y^2 , are unequal, the distributions are referred to as the elliptical distributions and 'distribution ellipses' with the oriented major and minor axes can be found in the (x, y) plane. These ellipses are ones defined as loci of constant distribution density [$f(x, y) = \text{constant}$] in the (x, y) plane and represent boundaries within which specified percentage of the collective is to be found.

In the case of elliptical distribution it is always possible to transform the components x and y to new orthogonal components ξ and η in which component correlation $r_{\xi\eta}$ is reduced to zero.

For this, it is only necessary to make the rotation transformation of the components ξ and η . The necessary angle of rotation, ϕ , is given by

$$\tan 2\phi = \frac{2\rho\sigma_x\sigma_y}{\sigma_x^2 - \sigma_y^2} \quad (3)$$

and the component ξ and η are related to x and y as

$$\left. \begin{aligned} \xi &= x \cos \phi + y \sin \phi \\ \eta &= -x \sin \phi + y \cos \phi \end{aligned} \right\} \quad (4)$$

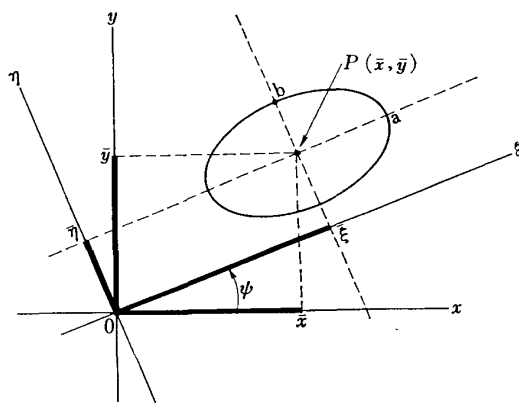


FIG. 2. Generalized elliptical bivariate distribution

Therefore, in the new coordinate system $O-\xi\eta$ (Fig. 2) the probability density function $f(\xi, \eta)$ is represented by

$$f(\xi, \eta) = \frac{1}{2\pi\sigma_\xi\sigma_\eta} \exp \left[-\frac{1}{2} \left\{ \left(\frac{\xi - \bar{\xi}}{\sigma_\xi} \right)^2 + \left(\frac{\eta - \bar{\eta}}{\sigma_\eta} \right)^2 \right\} \right] \quad (5)$$

Since equation (1) and (5) are equal over the same region of integration, following relationships can be obtained:

$$\sigma_\xi\sigma_\eta = \sigma_x\sigma_y\sqrt{1-\rho^2} \quad (6)$$

$$\sigma_\xi^2 + \sigma_\eta^2 = \sigma_x^2 + \sigma_y^2 \quad (7)$$

The probability that x and y (or ξ and η) will be found in a region S is given by

$$P(\xi, \eta) = P(x, y) = \frac{1}{2\pi\sigma_\xi\sigma_\eta} \iint_S \exp \left(-\frac{\lambda^2}{2} \right) d\xi d\eta \quad (8)$$

where

$$\lambda^2 = \frac{(\xi - \bar{\xi})^2}{\sigma_\xi^2} + \frac{(\eta - \bar{\eta})^2}{\sigma_\eta^2} \quad (9)$$

2.2 Confidence Ellipses

Since the right hand side of equation (9) is interpreted as the sum of squares of

two standardized normal biases, λ^2 obeys χ^2 -distribution with a degree of freedom 2. Then, if the ellipse expressed by equation (9) with $\lambda^2 = \chi^2(2; P)$ is drawn, the probability with which a point (x, y) , or, (ξ, η) falls in the ellipse becomes $100(1-P)\%$.

In the case of our interest, however, population parameters are not given. In this situation these parameters must be replaced with the sampling statistics $\bar{x}, \bar{y}, s_x, s_y, r$ or $\bar{\xi}, \bar{\eta}, s_\xi, s_\eta$, and Hotelling's T^2 must be used instead of χ^2 -distribution. Hotelling's T^2 is expressed by the following equation:

$$T^2 = \frac{2(N-1)}{N-2} F(2, N-2; \alpha) \quad (10)$$

where F denotes F -distribution described below and N is the sample size.

Probability density function of F -distribution with degrees of freedom ϕ_1, ϕ_2 is given by

$$f(x) = \frac{1}{B\left(\frac{\phi_1}{2}, \frac{\phi_2}{2}\right)} \left(\frac{\phi_1}{\phi_2}\right)^{\phi_1/2} x^{\phi_1/2-1} \left(1 + \frac{\phi_1}{\phi_2} x\right)^{-(\phi_1+\phi_2)/2} \quad (11)$$

where $B(p, q)$ is a beta function defined as follows:

$$B(p, q) = \int_0^1 t^{p-1} (1-t)^{q-1} dt \quad (12)$$

The value of F -distribution, $F(\phi_1, \phi_2; P)$, is defined by the following formula;

$$1-P = \int_0^{F(\phi_1, \phi_2; P)} f(x) dx \quad (13)$$

Equation (13) expresses the relation that the probability of stochastic variable obeying F -distribution to exceed the value of $F(\phi_1, \phi_2; P)$ is P .

In the case of Hotelling's T^2 , following expression is obtained by equations (10)–(13), since one of the degrees of freedom, ϕ_2 , is equal to 2:

$$T^2 \equiv \frac{2(\phi_2-1)}{\phi_2-2} F(2, \phi_2-2; P) = (\phi_2-1)(P^{-2/(\phi_2-2)} - 1) \quad (14)$$

Thus Hotelling's T^2 acquires following simplified representation:

$$T^2 = (N-1)(P^{-2/(N-2)} - 1) \quad (15)$$

As for the sampling data, following expressions can be obtained:

$$\frac{(x-\bar{x})^2}{s_x^2} - 2r \frac{(x-\bar{x})(y-\bar{y})}{s_x s_y} + \frac{(y-\bar{y})^2}{s_y^2} = (1-r^2)(N-1)(P^{-2/(N-2)} - 1) \quad (16)$$

or

$$\frac{(\xi-\bar{\xi})^2}{s_\xi^2} + \frac{(\eta-\bar{\eta})^2}{s_\eta^2} = (N-1)(P^{-2/(N-2)} - 1) \quad (17)$$

If the ellipse expressed by the equations (16) or (17) is drawn, this ellipse shows the confidence ellipse in which the 100 (1-P) % data exist among the total collective. Semimajor and semiminor axes, a and b are given as follows:

$$\left. \begin{aligned} a &= \sqrt{\lambda_1 T^2} \\ b &= \sqrt{\lambda_2 T^2} \end{aligned} \right\} \quad (18)$$

where

$$\left. \begin{aligned} \lambda_1 &= \frac{1}{2} [s_x^2 + s_y^2 + \sqrt{(s_x^2 + s_y^2)^2 - 4(s_x^2 s_y^2 - s_{xy}^2)}] \\ \lambda_2 &= \frac{1}{2} [s_x^2 + s_y^2 - \sqrt{(s_x^2 + s_y^2)^2 - 4(s_x^2 s_y^2 - s_{xy}^2)}] \end{aligned} \right\} \quad (19)$$

The slope of major axis is given by

$$\tan \phi = \frac{\lambda_1 - s_x^2}{s_{xy}} \quad (20)$$

2.3 Test of Noncorrelation

To measure the degree of circularity of the population distribution, test of non-correlation ($\rho=0$) must be applied to the value r obtained from the sampled data.

It is the prevailing fact that the following statistic t_0 obeys t -distribution with the degree of freedom $N-2$ if the correlation coefficient of the population is equal to zero ($\rho=0$):

$$t_0 = \frac{r\sqrt{N-2}}{\sqrt{1-r^2}} \quad (21)$$

where N is the sample size.

And hence if we set $\rho=0$ as the null hypothesis (H_0) and α as the level of significance, the problem of test of noncorrelation can be described as follows:

$$H_0: \rho=0 \quad R: t_0 \geq t(N-2; \alpha) \quad (22)$$

Thus to test $H_0: \rho=0$, t_0 must be calculated by equation (21) and, if $t_0 \geq t(N-2; \alpha)$, H_0 may be rejected with the level of significance α and correlation is regarded to exist between two components.

2.4 Problem from the Viewpoint of Range Safety

From the standpoint of range safety, the problem of our particular interest may be an estimation of the percentage of occurrence that the dispersion vector of the impact point of a rocket is equal to or less than a stated value. This problem is illustrated in Fig. 3. Here the shaded circle encompasses the desired percentage that dispersion vectors are equal to or less than a specified value.

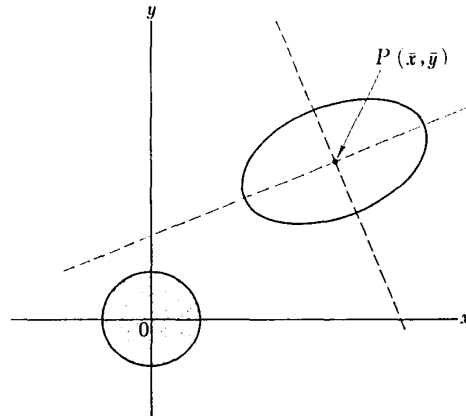


FIG. 3. Illustration from the standpoint of range safety problem

3. RESULTS AND DISCUSSION

3.1 Data Source, Scatter Diagram and Estimates of Parameters

Application of the foregoing vector statistics is now shown by use of data obtained from Table 1. Table 1 is a reproduction from impact point data of

TABLE 1. Data source

		Range	Types of rockets	Predicted range	Sample size N
A	Small rockets	Short	Single stage (S-, PT-, MT-, IT-types) First stage of multistage (K-, L-types)	0~300 km	55
B	Large rockets	Long	Second or upper stages of K-, L-types	300~3000 km	33
C	Total		Total of A and B	0~3000 km	88

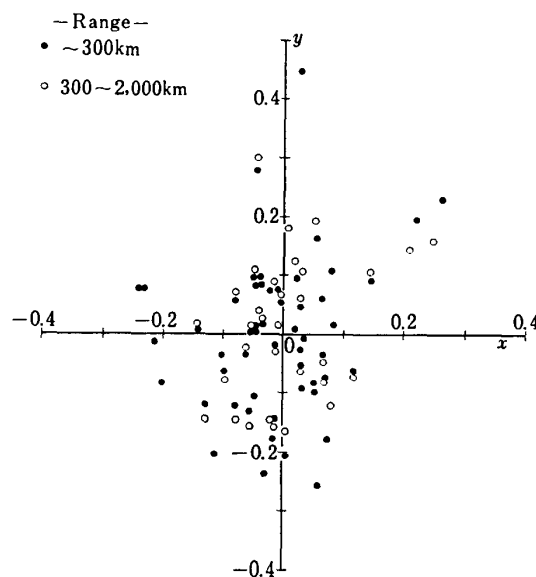


FIG. 4. Scatter diagram of impact point distributions

rockets launched at KSC since 1967 till 1974. Plotted in Fig. 4 is the impact point distribution of these rockets as nondimensionalized by their respective predicted ranges. From this figure, roughly speaking, elliptical binormal distribution may be assumed to be adequately fitted to the impact point distribution. Table 2 provides a listing of some computed estimates of statistical parameters.

TABLE 2. Some estimates of statistical parameters

	Range	\bar{x}	\bar{y}	s_x	s_y	s_{xy}	r	ϕ
A	Short	-0.009289	-0.002653	0.09875	0.12978	0.001988	0.1551	-14.64°
B	Long	0.005369	0.005413	0.08701	0.12057	0.002841	0.2709	-19.60°
C	Total	-0.003898	-0.000314	0.09435	0.12582	0.002300	0.1938	-16.79°

3.2 Confidence Ellipse and Test of Noncorrelation

Table 3 shows semimajor and semiminor axes of confidence ellipse according to the various percentage levels. These are illustrated in Fig. 5. Shown in Fig. 6 are these homothetic ellipses together with the impact point data.

TABLE 3. Semiaxes of confidence ellipses

			Confidence probability						
			25%	75%	90%	95%	97.5%	99%	99.5%
A	Small rockets	a	0.1012	0.2390	0.2916	0.3350	0.3744	0.4220	0.4588
		b	0.0738	0.1743	0.2126	0.2443	0.2731	0.3078	0.3324
B	Large rockets	a	0.0966	0.2157	0.2824	0.3259	0.3656	0.4150	0.4503
		b	0.0627	0.1401	0.1834	0.2117	0.2375	0.2695	0.2925
C	Total	a	0.0982	0.2170	0.2812	0.3220	0.3588	0.4033	0.4343
		b	0.0487	0.1529	0.1982	0.2270	0.2529	0.2842	0.3061

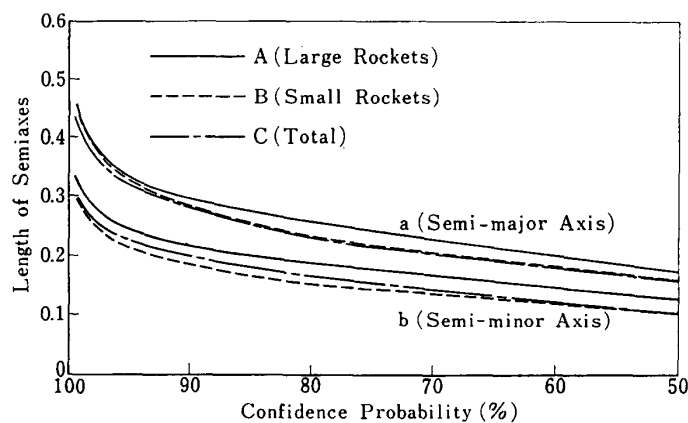


FIG. 5. Length of semiaxes of confidence ellipses

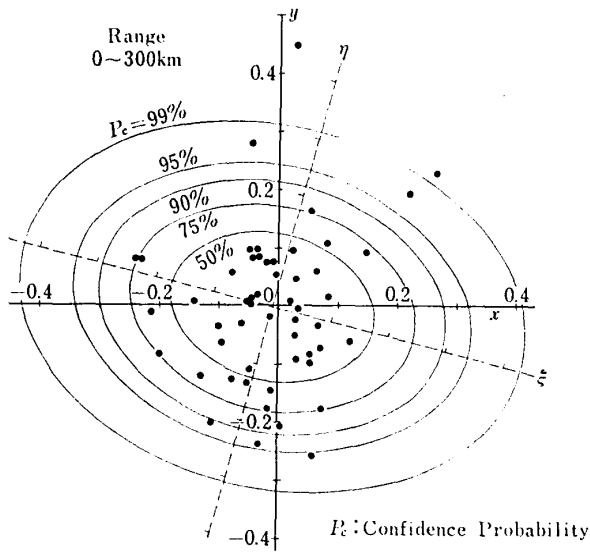


FIG. 6. Confidence ellipses

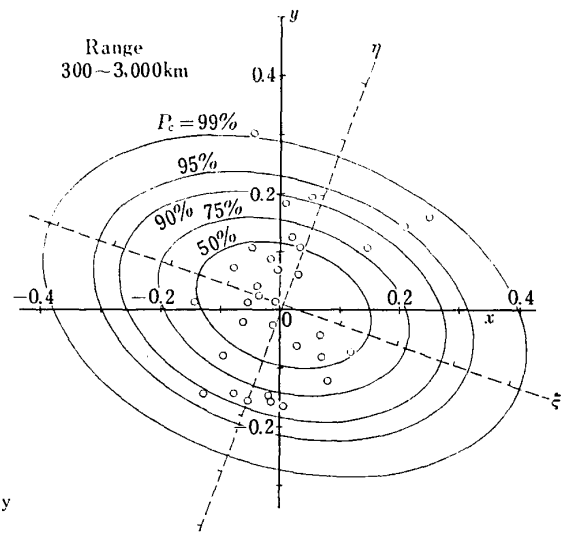


FIG. 6. Continued

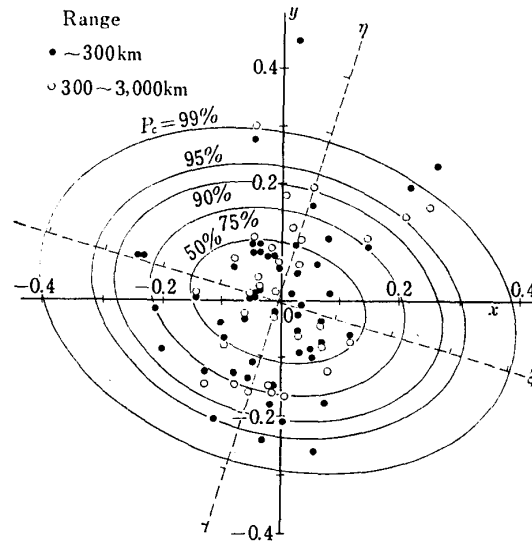


FIG. 6. Concluded

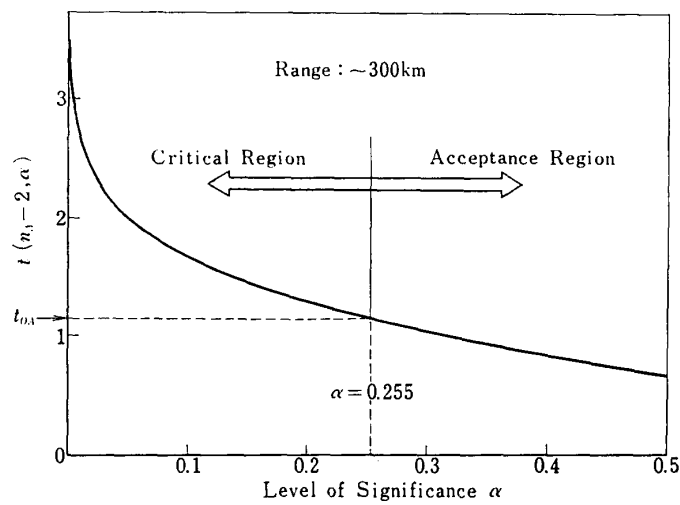


FIG. 7. Test of noncorrelation

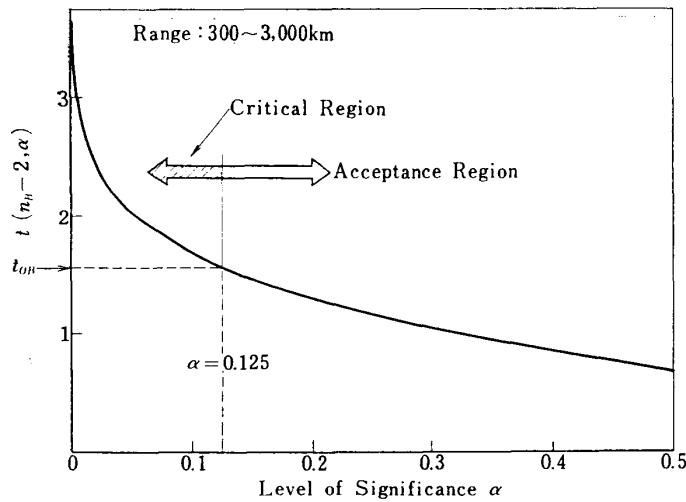


FIG. 7. Continued

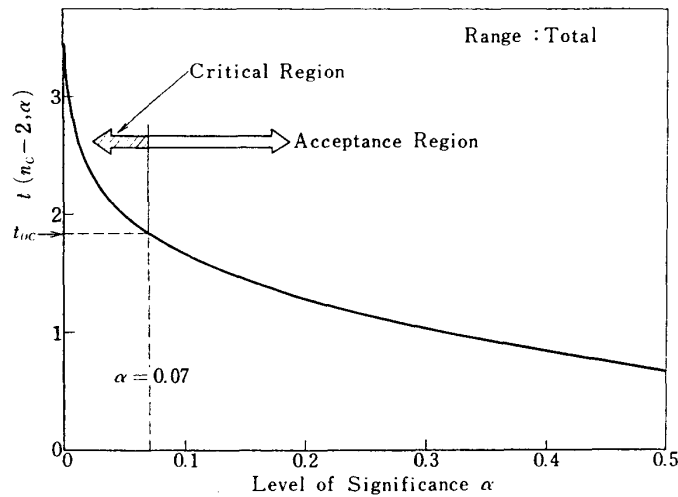


FIG. 7. Concluded

The result of test of noncorrelation is illustrated in Fig. 7 for several significance levels. In this figure, n_A , n_B , n_C denote respective sample sizes of A, B, C cases (cf. Table 1).

Thus for the distribution of impact points of rockets launched at KSC, the assumption of circularity is shown to be valid if the level of significance is carefully chosen.

3.3 Computation Related to the Width of Impact Zone

The problem illustrated in Fig. 3 is now treated. The answer sought is the percentage of occurrence that a dispersion vector does not exceed a stated value. To solve this problem equation (8) must be integrated over the circle with a specified radius, centered at the origin. The integration may be accomplished efficiently by use of a polar coordinate system (See reference [3]).

Results are given in Fig. 8, in which results obtained by circular distribution method and the empirical cumulative frequency method are also shown (descrip-

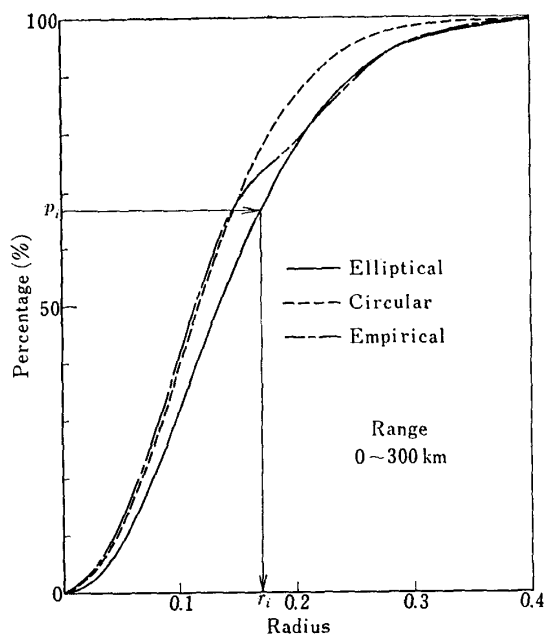


FIG. 8. Percentage of occurrence that a dispersion vector does not exceed a specified radius

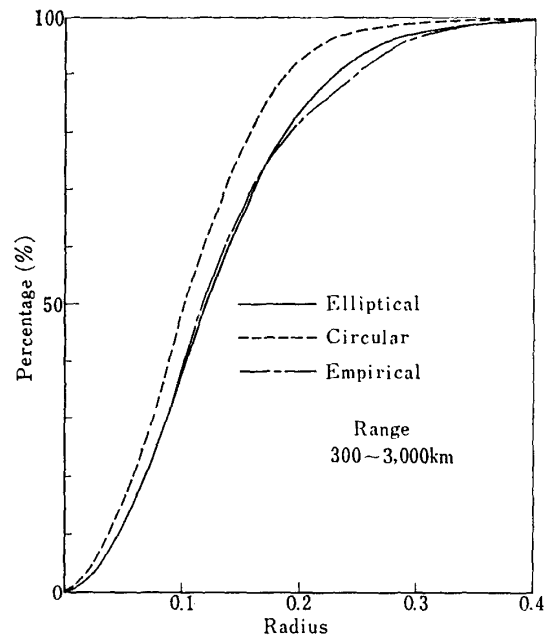


FIG. 8. Continued

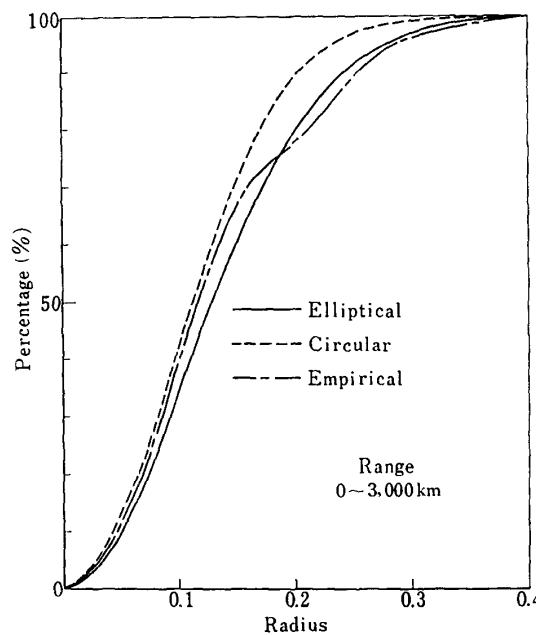


FIG. 8. Concluded

tion of circular distribution method is also shown in reference [3]). Probability levels for various radii determined by three methods are in fair agreement for both small and large rockets. Thus the assumption of circularity is again shown to be fairly valid as to the impact point distribution at KSC.

From the standpoint of range safety, Fig. 8 can be utilized to determine the radii of impact zones. In the case where the percentage of hitting the impact zone is assumed to be p_i nondimensionalized radius of the zone r_i can be obtained

from the figure. If the predicted impact range is denoted by R_0 , the radius of impact zone R_i can be determined as follows:

$$R_i = r_i R_0 \quad (23)$$

4. CONCLUSION

Statistical analysis was applied to data of impact points of rockets launched at KSC. Elliptical bivariate distribution method was shown to be valid for the impact point distribution at KSC. Circular distribution was also shown to be valid. Some computations indispensable for determining the width of impact zone were accomplished and useful results were obtained.

ACKNOWLEDGEMENT

The authors are much indebted to the members of rocket group in ISAS for permission to utilize impact point data. They also wish to express their gratitude for the encouragement received from Dr. D. Mori and Dr. T. Nomura. Acknowledgement also is due to Mrs. M. Mori for typewriting the manuscript.

The problem of separating the contribution of vehicle misalignment to impact point dispersion from the contribution of wind was not treated here but is being pursued by the authors and will be reported on later.

*Department of Space Technology
Institute of Space and Aeronautical Science
University of Tokyo
October 30, 1974*

REFERENCES

- [1] Crutcher, H. L. and Baer, L., "Computations from Elliptical Wind Distribution Statistics," J. of Appl. Meteor., Vol. 1, 1962.
- [2] Weaver, W. L., Swanson, A. G. and Spurling, J. F., "Statistical Wind Distribution Data for Use at NASA Wallops Station," NASA TN D-1249, July, 1962.
- [3] Matogawa, Y., "Statistical Distribution of Wind at KSC," ISAS Rept. No. 519, 1974.